Materials Today Communications 31 (2022) 103791

Contents lists available at ScienceDirect

Materials Today Communications

journal homepage: www.elsevier.com/locate/mtcomm

Preparation and characterization of curcumin and pomegranate peel extract chitosan/gelatin-based Films and their photoinactivation of bacteria

Lucas D. Dias [a,*], Mirella Romanelli V. Bertolo [b], Fernanda Alves [b], Clara M.G. de Faria [a], Murilo Álison V. Rodrigues [b], Letícia Keller B.C. Lopes [a], Ana Maria de Guzzi Plepis [b], Luiz Henrique C. Mattoso [c], Stanislau Bogusz Junior [b], Vanderlei S. Bagnato [a,d]

[a] São Carlos Institute of Physics, University of São Paulo, São Carlos 13566-590, SP, Brazil
[b] University of São Paulo, São Carlos Institute of Chemistry, São Carlos 13566-590, SP, Brazil
[c] Nanotechnology National Laboratory for Agriculture (LNNA), Embrapa Instrumentation, São Carlos 13560-970, Brazil
[d] Hagler Fellow, Department of Biomedical Engineering, College Station Texas, Texas A&M University, 77843, USA

ARTICLE INFO

Keywords:
Chitosan
Curcumin
Pomegranate peel extract
Films
Antimicrobial material
Antimicrobial photodynamic therapy

ABSTRACT

The development of photoantimicrobial films for food and medical devices decontamination is a continuous challenge. In this work, chitosan/gelatin-based films containing curcumin and pomegranate peel extract in different concentrations (0.5–5.0 mg photosensitizer g^{-1} solution) were prepared and characterized by ultraviolet–visible spectroscopy, fluorescence spectroscopy, infrared spectroscopy and scanning electron microscope; their structural morphology (thickness and moisture content, solubility and swelling degree, and opacity) was also analyzed. The photobleaching results (up to 90%) demonstrated a potential application of the films in antimicrobial photodynamic therapy (aPDT). In the antimicrobial tests, the films displayed a significant photoantimicrobial effect reducing *Staphylococcus aureus* up to 4 log units, using a light source at 450 and 525 nm (50 J cm^{-2}) for curcumin and pomegranate peel extract films, respectively. The results of this work open way for future development of photoantimicrobial films based on natural polymers, containing photosensitizers, for medical devices (e.g.: endotracheal tubes and catheters) and food packaging.

1. Introduction

Pathogenic microorganisms are a serious problem worldwide specially in food industry and hospital environment [1,2]. Due to food contamination, around one third of all food produced globally is discarded annually [3,4], resulting in a waste of 1.3 billion tons of food and thousands of hospitalization by ingestion of contaminated food [5–7]. Moreover, in the hospital environment, contaminations by microorganisms are responsible for infections related to the use of medical devices and implants, such as catheters and prosthetic joints, endotracheal tubes and endoscopes [8,9].

Considering the threat that these contaminations can pose, there is an urgent need to develop strategies to combat pathogenic microorganisms. In this sense, antimicrobial photodynamic therapy (aPDT) has gained scientific and pratical repercussion due to its high precision, non-invasiveness, high efficiency, controllability, possibility of repeating the treatment, low toxicity, in addition to its low cost [10,11]. Furthermore, aPDT has also shown to be a promising strategy for the microbial control of antibiotic and antifungal resistant microorganisms [12].

aPDT is based on the combined action of three essential elements: i) light; ii) molecular oxygen (O_2); and iii) a photosensitizing molecule (PS) [13], resulting on formation of reactive oxygen species (ROS) such as hydrogen peroxide (H_2O_2), superoxide ion ($O_2^{\cdot-}$), hydroxyl radical ($^{\cdot}OH$) and singlet oxygen ($^1O_2$), which leads to microorganisms inactivation [14,15]. In the recent years, some studies reported [16–18] the development of photosensitizers-functionalized biopolymers as innovative and efficient films to reduce food loss, such as strawberries, tomatoes, apricots, [19] and also for decontamination of medical materials. Among the biopolymers used, chitosan stands out due to its great versatility and antimicrobial properties [20–22]. Different molecules including gelatin can be incorporated into chitosan in order to increase the solubility of hydrophobic photosensitizers added to the polymeric network [23–27]; the improvement in the solubility allows these molecules to reach the desired targets, in this case,

* Correspondence to: São Carlos Institute of Physics, University of São Paulo, CEPOF, Av.Trabalhador Sancarlense, 400 - Centro, São Carlos, SP, Brazil.
E-mail address: lucas.dias1@usp.br (L.D. Dias).

https://doi.org/10.1016/j.mtcomm.2022.103791
Received 5 January 2022; Received in revised form 3 June 2022; Accepted 4 June 2022
Available online 8 June 2022
2352-4928/© 2022 Elsevier Ltd. All rights reserved.

microorganisms [28]. Therefore, active films incorporating natural antibacterial agents have been lately developed, namely pomegranate peel extract [29,30], lemongrass (Cymbopogon commutatus) essential oil [31], and natamycin [32].

Herein, chitosan/gelatin films functionalized with curcumin and pomegranate peel extract as photosensitizers in different concentrations (0.5–5.0 mg photosensitizer g^{-1} solution) were prepared and characterized by scanning electron microscope (SEM), UV–vis, fluorescence, and infrared spectroscopies. Photobleaching, photostability, in vitro photosensitizers release, antioxidant properties, and antimicrobial photodynamic tests with the developed films were conducted. The main purpose of this work is to demonstrate that photosensitive chitosan/gelatin films containing natural photosensitizing molecules like curcumin and pomegranate peel extract may be an efficient approach for the bacterial photoinactivation opening ways for photodecontamination of medical devices surfaces and food packaging.

2. Experimental

2.1. Chemicals and solvents

Chitosan (poly-D-glucosamine, high molecular weight, 310 000–375 000 Da, obtained from deacetylated chitin, > 75% deacetylated) was purchased from Sigma-Aldrich and used without any purification process; gelatin was also obtained from Sigma-Aldrich, as a powder with gel strength of ~300 g bloom, type A, from porcine skin. Curcumin (purity >99%) was obtained from PDT Pharma (Cravinhos, São Paulo, Brazil). Pomegranates fruits were obtained in local commerce in the city of São Carlos, SP, Brazil. After washing, the fruits were manually peeled, and the peels were dried in an Edwards Freeze Dryer - Modulyo model (Edwards High Vacuum International, West Sussex, United Kingdom).

2.2. Pomegranate peel extraction

Pomegranate peel extract was obtained according to the procedure described by Bertolo et al. (2021) [33]: the dried peels were crushed with a blender to obtain a thin powder; then, the powder was extracted with a hydroethanolic solution (60% EtOH, v/v), in the ratio of 1 g of powder to 30 g of solvent, at 45 °C for 1 h, in an ultrasonic bath (Unique USC-1400A, Indaiatuba, SP, Brazil). After extraction and ethanol evaporation for 48 h under air flow, the extract was lyophilized for 48 h to obtain a thin, dry, and reddish powder, with a 54% yield. The extract was stored at 4 °C and protected from light until its use.

2.3. Films preparation

For films preparation, the initial solutions of chitosan (CH) and gelatin (G), both at 1% (w/w), were prepared as follows: chitosan was solubilized in lactic acid 1% (w/w) for 24 h, at room temperature, and gelatin was solubilized in water, at 60 °C for 30 min, followed by gelation at 4 °C for 2 h [33]; the mixture of these solutions, in the proportion of 80% of CH and 20% of G, led to CHG solution, i.e., without any photosensitizing molecules.

For curcumin (C) and pomegranate peel extract (E) incorporation, the photosensitizers were solubilized in ethanolic solutions (70% EtOH, v/v) at the concentrations of 100 mg mL^{-1} and 250 mg mL^{-1}, respectively. Then, the photosensitizers solutions were slowly dripped into CH solution, under stirring at 45 °C, until homogeneous mixtures (i.e., without the presence of visible precipitates) were obtained. Finally, G was added to the mixtures, to complete the film-forming solutions. The proportion adopted between the polymers and the photosensitizers was of 1 mL of C or E solution /50 g of CHG. In total, six film-forming solutions were prepared, named: CHGC0.5, CHGC1, CHGC2 (final concentrations of 0.5, 1 and 2 mg curcumin g^{-1} solution), CHGE1, CHGE2, and CHGE5 (final concentrations of 1, 2 and 5 mg pomegranate peel extract g^{-1} solution). The solutions were used in the antioxidant tests described below and placed in Teflon® molds for the casting procedure (room temperature, one week), to obtain films.

2.4. Structural morphology of films

2.4.1. Thickness and moisture content

Thickness of films was measured at 10 random positions with a micrometer M110–25 (Mitutoyo Mfg. Co., Japan). Their moisture content was determined by the difference in weight before and after drying at 80 °C for 24 h. All the analysis regarding films characterization were carried out in triplicate for each sample.

2.4.2. Solubility and swelling degree

After drying at 80 °C for 24 h, the films were placed in a desiccator with sodium hydroxide and weighed after stabilization (*W1*); then, the films were placed in 10 mL of water and left stirring at room temperature, for 6 h. In specific time intervals (30 min, 1 h, 2 h, 4 h, and 6 h), the swollen films were weighed (*W2*) and returned to the water. After 6 h, the films were placed to dry again at 80 °C for 24 h, and their final weight was measured (*W3*) [34]. The solubility and swelling degree (for each time interval adopted) of the films were calculated according to Eq. (1) and Eq. (2), respectively.

$$Solubility \quad (\%) = \left(\frac{W1 - W3}{W1}\right) x \quad 100 \tag{1}$$

$$Swelling \quad degree \quad (\%) = \left(\frac{W2 - W1}{W1}\right) x \quad 100 \tag{2}$$

2.4.3. Opacity

To determine the light barrier property of the films, the absorbance of rectangular film pieces was measured at 600 nm in a spectrophotometer test cell (U-300, HITACHI, Japan) [35]. The opacity (A mm^{-1}) was calculated with Eq. (3), where $Abs_{600\ nm}$ is the measured absorbance, and *L* is the films thickness (in mm).

$$Opacity = \frac{Abs_{600 \quad nm}}{L} \tag{3}$$

2.4.4. Scanning Electron Microscope (SEM)

SEM analysis were performed using a JSM-6510/GS scanning electron microscope (JEOL, Japan). To assess the cross-sectional surface, the samples were fractured and fixed onto 90° specimen stubs. The films were coated with a 5 nm layer of gold using a sputter coater and surfaces and cross-sectional surfaces were investigated with an accelerating voltage of 10 kV. The thickness and the roughness of the films were measured from SEM images using ImageJ software.

2.5. Optical/spectroscopic characterization

UV–vis analysis was performed using a Cary 5000 UV–vis–NIR spectrometer (Santa Clara, CA, United States). Fluorescence characterization was carried out using an Agilent Technologies Cary Eclipse Fluorimeter Spectrometer (Victoria, Australia). FT-IR characterization was carried out using an Agilent Cary 630 FTIR spectrometer (Santa Clara, CA, United States) between 400 and 4000 cm^{-1}, with a resolution of 8 cm^{-1}.

2.6. Photobleaching study of the films

The photobleaching experiment was carried out using a Biotable® apparatus (at 525 nm = 8.8 mW cm^{-2} and at 450 nm = 40 mW cm^{-2}) and the fluorescence of the films samples containing the pomegranate and curcumin extracts was measured with a Cary Eclipse fluorimeter (Victoria, Australia). The films were submitted to lights dosages, which started in 0 J cm^{-2} (without any light being applied), and increased by 25 J cm^{-2}, until the maximum of 100 J cm^{-2}. After each light dosage

the fluorescence was measured. For the photobleaching percentage, it was considered the decrease of fluorescence peak at 540 nm for the pomegranate and 420 for curcumin.

2.7. Photostability evaluation of the chitosan/gelatin matrix by FT-IR

The photostability experiment was performed under illumination using a LED apparatus (Biotable®, São Carlos, SP, Brazil), at 525 nm = 8.8 mW cm^{-2} and at 450 nm = 40 mW cm^{-2} for chitosan/gelation matrix containing pomegranate and curcumin, respectively. After irradiation (at 20 406 080 or 100 J cm^{-2}), FT-IR spectra of the films was obtained using an Agilent Cary 630 FTIR spectrometer with a resolution of 8 cm^{-1} between 400 and 4000 cm^{-1}.

2.8. In vitro photosensitizers leaching

The in vitro photosensitizers release from the films was evaluated placing them into an aqueous medium (pH = 7). At defined time intervals (0 h, 6 h, 12 h, 18 h and 24 h), fractions of 2 mL were taken for measurements by UV–vis spectrophotometry and replaced after the analysis. The concentration of photosensitizers was determined at 430 nm and 540 nm for curcumin and pomegranate peel extract, respectively. The amount of the photosensitizers released was calculated using a calibration curve.

2.9. Antioxidant evaluation of the films

2.9.1. Total phenolics content (TPC)

Curcumin and pomegranate peel extract, as well as the film-forming solutions of chitosan, gelatin, and the active compounds, were characterized regarding their total phenolic content (TPC), according to the Folin-Ciocalteu colorimetric method [36,37]. Ethanolic solutions (60%, v/v) of C and E were diluted in water at 100 μg mL^{-1}, and the film-forming solutions were diluted in water at 100 mg mL^{-1}. Each sample was placed to react with Folin's reagent (Sigma-Aldrich®), in the proportion of 1:1; the addition of 7% sodium carbonate (w/w) stopped the reaction after 5 min, and the absorbance was measured at 725 nm after 15 min, in a Thermo ScientificTM Multiskan GO UV-Vis spectrophotometer. The blank used was water, and a gallic acid calibration curve (y = 0,019x – 0065, R^2 = 0.9997) was applied to determine the TPC of the samples. The results were expressed in mg gallic acid equivalent (mg GAE) g^{-1} curcumin/extract or mg^{-1} film-forming solution.

2.9.2. DPPH scavenging activity

The antioxidant activity against the DPPH radical (2,2-diphenyl-1-picrylhydrazyl) was determined for C, E, and the chitosan/gelatin film-forming solutions [38]. The samples, at the same concentrations used in TPC analysis, were placed to react with a 0.01 mmol L^{-1} radical solution; the absorbance was measured after 30 min of reaction in a Thermo ScientificTM Multiskan GO UV-Vis spectrophotometer. The radical scavenging activity (RSA) percentage of each sample was determined with Eq. (4), where: Abs_{sample} is the final absorbance for each sample and Abs_{blank} is the DPPH absorbance, without any antioxidant specie, after 30 min

$$\% \quad RSA = \left(\frac{Abs_{blank} - Abs_{sample}}{Abs_{blank}}\right) \quad x \quad 100 \tag{4}$$

2.10. Antimicrobial photodynamic tests

Methicillin-sensitive *Staphylococcus aureus* (from American Type Culture Collection, number 25 923) stored at − 20 °C in tubes containing Tryptic Soy Broth (TSB, KASVI, São José dos Pinhais, PR, Brazil) with 50% glycerol was reactivated in Brain Heart Infusion (BHI) (KASVI, São José dos Pinhais, PR, Brazil) agar plates in incubator at 37 °C for 24 h. After reactivation, 5–10 colonies were suspended in a tube with 10 mL of TSB and the *S. aureus* was incubated at 37 °C for 16 h. An aliquot of 500 μL of the suspension was diluted in 9.5 mL of fresh TSB and incubated until the mid-log growth phase. The suspension was standardized at optical density of 0.2 arbitrary units (a.u.) (equivalent to 10^8 cells/mL), determined by UV–vis spectroscopy.

For the antimicrobial evaluation of the films, aliquots of 1 mL of the standardized bacteria suspension were transferred into a 24-wells plate. Then, samples of the films (5 mm × 5 mm) were immersed in the bacteria suspension during 10 min, for the bacteria adhesion onto the films. After this, the films were transferred to another 24-wells plate for the irradiation. Samples were illuminated in the LED device (450 or 525 nm) at the dose of 50 J cm^{-2}. After treatments, the viability assay was performed. For this, films were removed from the plate and inserted into tubes containing 1 mL of sterile saline. Then, tubes were vigorously vortexed for 30 s allowing the detachment of the cells. To determine bacteria survival, aliquots of the contents of each sample were serially diluted 10-fold in sterile saline. Duplicate 16.6 μL aliquots (total = 33.2 μL) were spread over the surfaces of BHI agar plates. All plates were aerobically incubated at 37 °C for 24 h. Then, the colony forming units (CFU/mL) were calculated. All values are represented as average ± SEM (standard error of the mean), which shows the standard deviation of the sample mean. All experiments presented were repeated at least six times with comparable results.

3. Results and discussion

3.1. Preparation of curcumin and pomegranate chitosan/gelatin-based films

The curcumin and pomegranate chitosan/gelatin-based films (CHGC0.5, CHGC1, CHGC2, CHGE1, CHGE2 and CHGE5) were prepared according to Section 2.3 using six film-forming solutions (Table 1) [33]. To obtain films (Fig. 1), the solutions were placed on Teflon® molds for the casting procedure.

3.2. Appearance, thickness, and moisture content

Table 2 summarizes the physicochemical properties of the chitosan and gelatin films containing pomegranate peel extract and curcumin, at different concentrations; film thickness ranged from 0.039 ± 0.008 mm (CHGE1) to 0.0515 ± 0.008 mm (CHGC1). In general, the incorporation of active compounds and the increase in their concentration led to thicker and more intensely colored films; such tendency was expected, due to the intense coloration of the photosensitizers solutions before their incorporation into the polymeric matrix. In the case of films containing curcumin, a greater heterogeneity was observed, probably associated with the higher hydrophobicity of curcumin and with its lower solubilization in the ethanolic solution, when compared to the pomegranate peel extract (Fig. 1). Factors such as stirring, temperature and speed of incorporation (dripping) of curcumin to the polymeric matrix, as well as the way in which the photosensitizer is incorporated (powder, in solution, nanostructured, in more concentrated or diluted solutions), will affect the final homogeneity of the films, and can be better evaluated and improved in future works. In the case of the films

Table 1
Composition of curcumin and pomegranate chitosan/gelatin-based films.

Samples	Composition
CHGC0.5	0.5 mg curcumin g^{-1} solution
CHGC1	1 mg curcumin g^{-1} solution
CHGC2	2 mg curcumin g^{-1} solution
CHGE1	1 mg promegranate peel extract g^{-1} solution
CHGE2	2 mg promegranate peel extract g^{-1} solution
CHGE5	5 mg promegranate peel extract g^{-1} solution

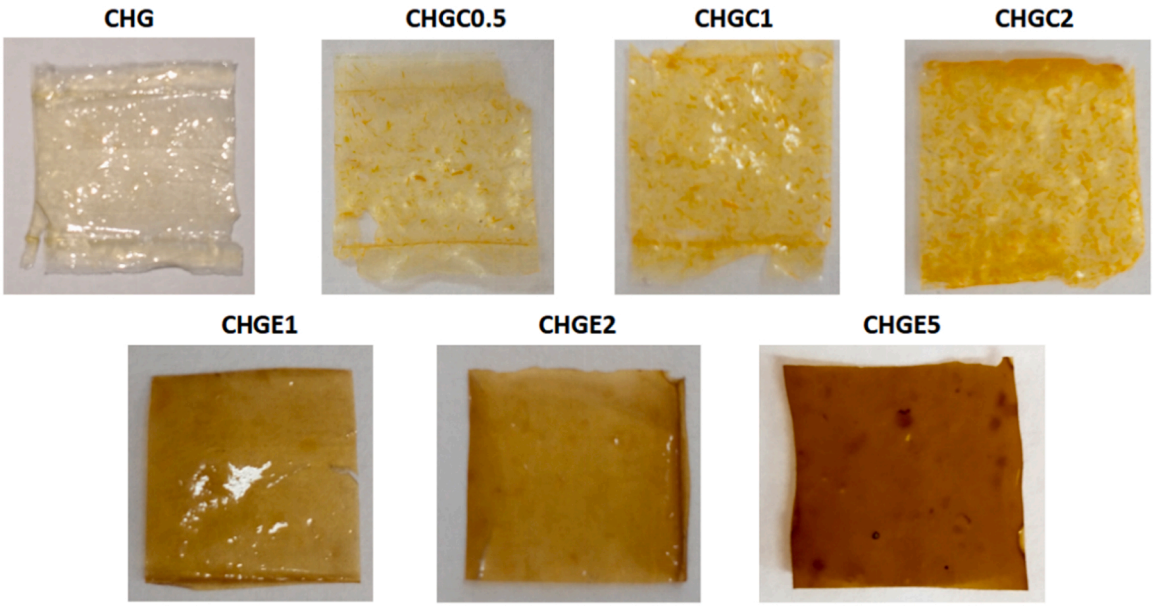

Fig. 1. Images of curcumin and pomegranate chitosan/gelatin-based films.

Table 2
Thickness, moisture content, solubility, swelling and opacity of chitosan and gelatin films containing pomegranate peel extract and curcumin at different concentrations.

Film	Thickness (mm)	Moisture (%)	Solubility (%)	Swelling* (%)	Opacity (A mm^{-1})
CHG	0.045 ± 0.006$^{a, b}$	8.41 ± 1.79^{a}	33.00 ± 5.90^{a}	2307 ± 465$^{a, b}$	7.95 ± 1.00^{c}
CHGE1	0.039 ± 0.008^{b}	7.73 ± 1.40^{a}	12.62 ± 1.23^{b}	857 ± 184^{b}	15.98 ± 1.26^{a}
CHGE2	0.041 ± 0.006$^{a, b}$	9.79 ± 1.95^{a}	13.76 ± 1.57$^{a, b}$	704 ± 187^{b}	14.14 ± 2.00$^{a, b}$
CHGE3	0.045 ± 0.012$^{a, b}$	10.87 ± 1.68^{a}	13.57 ± 2.36$^{a, b}$	553 ± 145^{b}	13.74 ± 0.83$^{a, b}$
CHGC0.5	0.040 ± 0.008^{b}	10.70 ± 2.24^{a}	16.55 ± 6.51$^{a, b}$	17 257 ± 8778^{a}	10.60 ± 0.85$^{b, c}$
CHGC1	0.051 ± 0.008^{a}	10.02 ± 1.33^{a}	20.80 ± 3.22$^{a, b}$	9061 ± 4848$^{a, b}$	13.57 ± 1.51$^{a, b}$
CHGC2	0.050 ± 0.006$^{a, b}$	11.49 ± 4.00^{a}	26.24 ± 9.03$^{a, b}$	4439 ± 723^{b}	16.70 ± 1.16^{a}

In the same column, values with the same superscript letter (a-c) indicate significantly equal samples ($p > 0.05$). *Values obtained after 1 h in water for CHGC0.5 and CHGC1, after 2 h in water for CHG and CHGC2, and after 6 h in water for CHGE1, CHGE2 and CHGE5.

containing pomegranate peel extract, only CHGE5 presented a more heterogeneous structure, which is related to the possible aggregation or saturation of the polyphenols at this high concentration. Regarding moisture content, all films had significantly equal water contents and not higher than 11.49%; moisture ranged from 7.73 ± 1.40% (CHGE1) to 11.49 ± 4.00% (CHGC2).

3.3. Solubility and swelling degree

The high solubility of polymeric films is one of their main obstacles when their application in food matrices and for medical devices is aimed; it is desirable that the films maintain their defined structure and integrity when in contact with water, without the release or loss of their active compounds. The incorporation of pomegranate peel extract was able to decrease the solubility of chitosan and gelatin films by approximately 20% (from 33.00 ± 5.90% in CHG to 12.62 ± 1.23% in CHGE1) (Table 1). This result is an indication of a greater interaction of the phenolic compounds in the extract with the polymeric chains of chitosan and gelatin, which makes the system more resistant to the solubility promoted by water [39]; the effect of the increase in the extract concentration, however, was not significant on the solubility of the films, which may be related to the stability of the polymeric matrix once the phenolic compounds started to interact with groups of both polymers.

The inclusion of curcumin also led to lower solubility values when compared to the CHG control film, but in this case the films were more susceptible to disintegration and loss of their defined structure after 2 h in water. The increase in curcumin concentration from CHGC0.5 to CHGC2 led to a tendency towards a gradual increase in the solubility of the films (from 16.55 ± 6.51% in CHGC0.5 to 26.24 ± 9.03% in CHGC2). This opposite effect to that observed for the pomegranate peel extract is related to the greater hydrophobicity of the curcumin molecule, which led to more heterogeneous films and, consequently, less stable in solution [31]. Thus, the polymers have greater freedom to interact with water and, consequently, the solubility of the films increased.

Regarding swelling, the films showed a water absorption profile after 30 min; CHGC0.5 and CHGC1 films lost their defined film integrity after 1 h in water, due to their high swelling capacity. CHGC2 swelled less, probably due to the higher concentration of curcumin, which led to a greater number of interactions between the photosensitizer and the polymers and, consequently, to a lower diffusion capacity of water molecules though the polymeric matrix. The same happened for CHG film, which swelled around 2307 ± 465% after 2 h. The films containing pomegranate peel extract remained intact throughout the analysis, without loss of structure, and with %'s of swelling significantly lower than those observed for the CHG and CHGC films; again, the poor stability of the films containing curcumin can explain this result, since they lost their defined structure during swelling, unlike the films containing the extract. Finally, the increase in extract concentration led to a gradual decrease in the swelling capacity of the films, with CHGE5 being the film with the lowest % of swelling at the end of the 6 h of analysis (553 ± 145%) (Table 1).

3.4. Opacity

Opacity is one of the light barrier properties that must be carefully evaluated when dealing with active films with potential application as coatings; it is expected that the presence of phenolic compounds from

pomegranate peel and curcumin leads to greater opacity of polymeric films, related to greater absorption of UV–vis radiation due to the unsaturated bonds in their structures (C═C, C═O, C═N). Thus, the films can act as a barrier to the passage of light, reducing or delaying light-induced oxidative processes [40].

There was a significant increase in the opacity of the CHG film (7.95 ± 1.00 A mm^{-1}) after the addition of the active compounds (Table 2); the nature of the active compound did not affect the opacity of the films, as the films containing pomegranate peel extract and films containing curcumin showed significantly equal opacity values. Regarding the concentration of the photosensitizers in the films containing curcumin, the increase in pigment concentration from CHGC0.5 to CHGC2 led to a tendency towards an increase in opacity values (from 10.60 ± 0.85–16.70 ± 1.16 A mm^{-1}).

3.5. Scanning electronic microscopy (SEM)

SEM images of surface and fractures of films are shown in Fig. 2(a-g) and Fig. 2(h-n), respectively, while their thickness values are shown in Table S1 and the roughness profiles obtained by SEM images analysis are shown in Fig. S5. Although atomic force microscopy is a more appropriate technique to measure the roughness of samples, the analysis of uniformity in SEM surface images aims to clarify the differences in smoothness between the samples according to the incorporation of different contents of extracts. CHG film presented a flat and smooth surface (Fig. 2a and S5a) and a compact structure without aggregates or phase separation (Fig. 2h). The inclusion of curcumin or pomegranate peel extracts affected differently films morphology. While curcumin extract incorporation resulted in aggregates that increased with curcumin contents (Fig. 2(b-d and i-k and S5 (b, d, f)), pomegranate peel extract addition affected mainly films surfaces (Fig. S6), as shown in highlights of (Fig. 2(e-g)), with the increase in pomegranate extract content resulted in less smooth films surfaces, similar to the results reported by Soltanzadeh et al. [29]. Due to the high hydrophobicity of curcumin extract [41], when incorporated in the aqueous polymer solutions this extract tends to agglomerate, resulting in particles apparent in both surface and cross-sectional images, as previously reported for chitosan films incorporated with different contents of curcumin grafted cellulose nanofiber [42]. Aggregates of pomegranate extract, however, are only visible in CHGE5 fracture image (Fig. 2n) and the greater

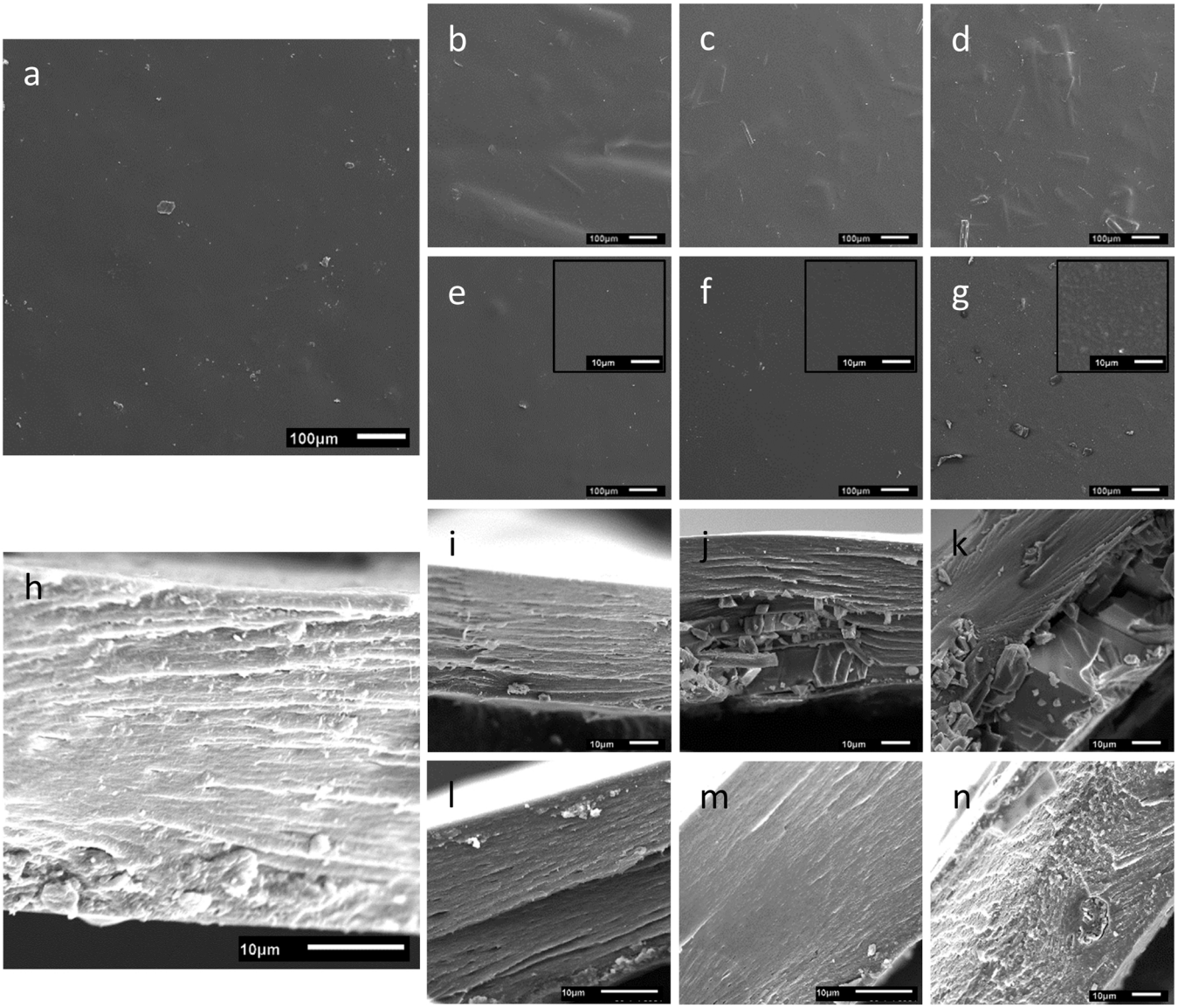

Fig. 2. SEM images of surface and cross-sectional surfaces for CHG (a and h), CHGC0.5 (b and i), CHGC1 (c and j), CHGC2 (d and k), CHGE1, (e and l), CHGE2 (f and m) and CHGE5 (g and n) at 100 and 1000–2000 X magnifications, respectively. Highlighted in images e-g are surface images with 1000X magnification.

miscibility of this extract in comparison to the curcumin can be explained by the hydrophilic nature of many of the polyphenolic compounds that compose it [43].

The increase in both extracts content resulted in thicker films, except for CHGE1, that probably became thinner due to an increase in the interactions between the polyphenol compounds and polymers at this concentration, compacting this film.

3.6. Optical/spectroscopic characterization

Figs. S1 and S2 present the UV–vis spectra of curcumin and pomegranate peel extract showing typical maximum absorptions at 430 and 545 nm, respectively. In Fig. 3, the fluorescence emission spectra of CHG (black line), CHGC0.5 (red line), CHGC1 (blue line), and CHGC2 (green line) are presented, with excitation at 430 nm. The fluorescence spectra of CHGC0.5, CHGC1, and CHGC2 are similar to that of the curcumin with an emission wavelength range (510–600 nm) while the spectrum of the CHG does not show any fluorescence emission. Thus, qualitative analysis of the fluorescence emission spectra of the photosensitizers-functionalized films (CHGC0.5, CHGC1, and CHGC2) evidence that the energy of the excited state of curcumin is not changed by the presence of the biopolymer matrix.

Figs. 4a and 4b show the FT-IR spectra of the curcumin and pomegranate chitosan/gelatin-based films, respectively. Due to the similar functional groups present in chitosan and gelatin molecular structure, there are numerous similar peaks observed in FTIR spectra. From the analysis of spectra of the curcumin-chitosan/gelatin films (Fig. 4a), all spectra show the following bands: 2924 cm^{-1} (CH antisymmetric and symmetric stretching, presented in chitosan and gelatin), 2857 cm^{-1} (CH antisymmetric and symmetric stretching), 1732 cm^{-1} (C═O stretch/hydrogen bond coupled COO^- (amide carbonyl group (amide I), observed in chitosan), 1564 cm^{-1} (NH bend coupled with CN stretch (amide group - amide II), observed in chitosan), 1462 cm^{-1} (CH_2 bending (scissors) vibration), 1375 cm^{-1} (CH_2 wag of proline and glycine), 1252 cm^{-1} (NH bend stretch coupled C–N stretch), 1027 cm^{-1} (C–O skeletal stretch), and C–H deformation vibration (carbohydrate). These bands observed are according to those described in the literature [25]. The FT-IR spectra of pomegranate chitosan/gelatin-based films (Fig. 4b) showed similar peaks as those observed for curcumin films (Fig. 4a). There was not observed typical peaks from curcumin and pomegranate peel extract, because of the low percentage of them (up to 2 mg and 5 mg g^{-1}, respectively) added to chitosan/gelatin matrix, as also observed by Ghaee [44]. Moreover, due to FT-IR customized the surface of the material, the existence of these peaks for chitosan and gelatin present a perfect combination of these two polymers and ionic interaction between chitosan (NH_3^+) and gelatin (COO^-), as described in the literature [45].

The photobleaching profile of the photosensitizers-functionalized

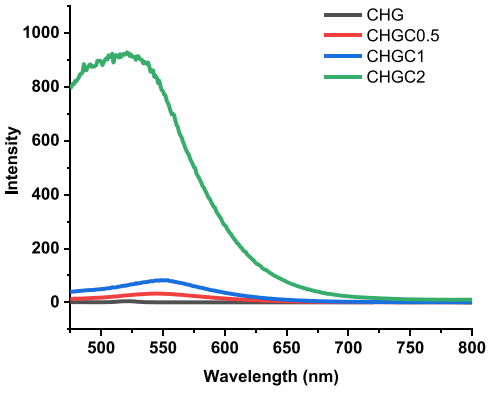

Fig. 3. Fluorescence spectra of: CHG, CHGC0.5, CHGC1, and CHGC2 with excitation at 430 nm.

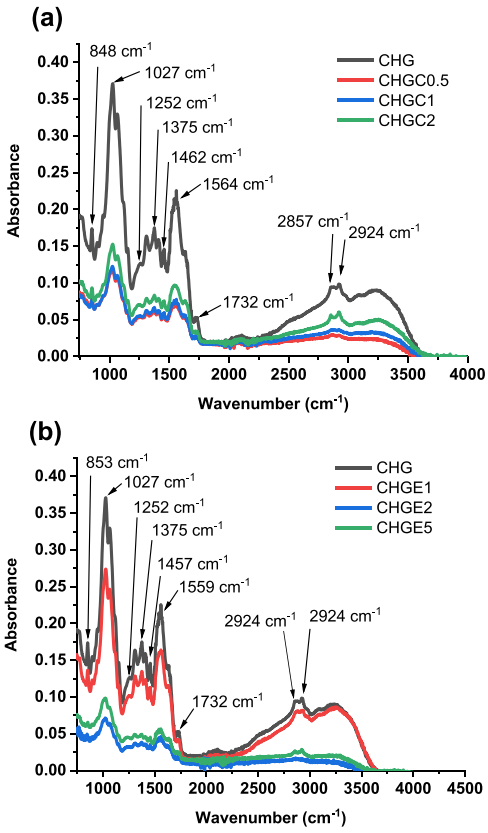

Fig. 4. FT-IR spectra of: a) CHG, CHGC0.5, CHGC1, CHGC2; b) CHG, CHGE1, CHGE2, and CHGE5.

chitosan/gelatin films was evaluated and described in Figs. 5a and 5b. Photobleaching is characterized by the loss of absorption or fluorescence of the photosensitizer under illumination. This photodegradation indicates the formation of reactive oxygen species ($^1O_2$, H_2O_2, $O_2^{\cdot-}$, $^{\cdot}OH$) opening perspectives for the use of the photosensitive materials in PDI [46,47]. The photosensitizers-functionalized films were submitted to irradiations at different light doses (255 075 and 100 J cm^{-2}) and fluorescence decay were analyzed at 420 and 540 nm for curcumin and pomegranate peel extract, respectively. Curcumin films (Fig. 5a) showed that photobleaching rate is light dose and concentration-dependent presenting a maximum photobleaching rate using 100 J cm^{-2} and a curcumin concentration at 2 mg g^{-1} of film (CHGC2). On the other hand, photobleaching analysis of the pomegranate peel extract films presented as light dose-dependent but a concentration-dependency was not observed (Fig. 5b). The CHGE5 (highest concentration for pomegranate peel extract) presented the lowest photobleaching profile compared to CHGE1 and CHGE2, which may be due to aggregation of the pomegranate peel extract on the biopolymer matrix (as observed in SEM images); such aggregation may have hampered the photobleaching profile of the extract, not making it so available in the polymeric matrix so that its irradiation was complete, regardless the dose tested.

Moreover, the physical structural of the films after illumination was evaluated by FT-IR. This technique has been used to detect structural changes on polymers surfaces by analyzing functional groups. From the analysis of FT-IR spectra (Figs. S3 a-g), it was not observed any modification of the spectra compared to the initial condition (before illumination), indicating that there was no structural modification with respect to functional groups on the polymer surface after irradiation with different light doses (0–100 J cm^{-2}).

3.6.1. In vitro photosensitizers leaching

Photosensitizers leaching of films (CHGC0.5, CHGC1, CHGC2,

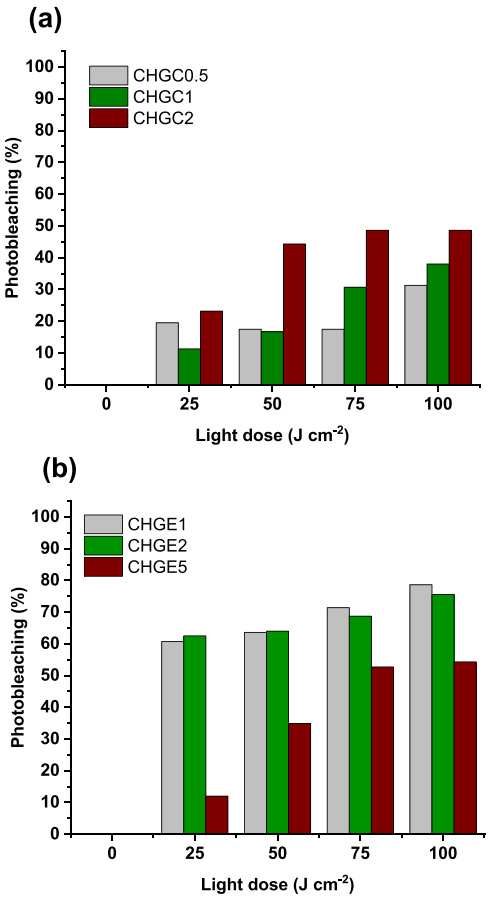

Fig. 5. Photobleaching profile of: a) CHG, CHGC0.5, CHGC1, CHGC2; b) CHG, CHGE1, CHGE2, and CHGE5. These experiments were performed using a light source at 450 and 525 nm for curcumin and pomegranate peel extract, respectively.

CHGE1, CHGE2 and CHGE5) was determined placing them into aqueous medium (pH = 7) and analyzed by UV-Vis at different times (0 h, 6 h, 12 h, 18 h and 24 h). The UV–vis spectra of CHGC0.5, CHGC1, CHGC2, CHGE1, CHGE2, and CHGE5 films are shown in Fig. S4. From the analysis of the UV–vis spectra (Fig. S4), curcumin and pomegranate peel extract leaching from functionalized-films was not observed displaying a great stability for future applications.

3.7. Antioxidant analysis

Fig. 6a shows the TPC determined for the pomegranate peel extract and for curcumin by the Folin-Ciocalteu method: while the extract presented an average TPC of 215.17 ± 5.27 mg GAE g^{-1}, curcumin had a lower phenolic content of around 4.82 ± 1.21 mg GAE g^{-1}. This result was already expected, since the chemical structure of synthetic curcumin has phenolic groups only at its extremities; pomegranate peel extract, in turn, is a mixture of several phenolic compounds, like gallic acid, caffeic acid, and punicalagin. The addition of these photosensitizers to chitosan and gelatin mixtures, as well as the increase in their concentration, led to a significant increase in the phenolic content of the film-forming solutions for CHGE1, CHGE2, and CHGE5 (Fig. 6b). All the film-forming solutions containing curcumin were significantly equal to CHG control solution.

The same tendency was observed in the % RSA results against the DPPH radical: Fig. 6c shows that the pomegranate peel extract, at the concentration of 100 μg mL^{-1}, was able to inhibit about 70.43 ± 1.25% of the radical in contact with it; curcumin, in turn, inhibited 17.61 ± 4.15%, at the same concentration. The addition of the extract, at all

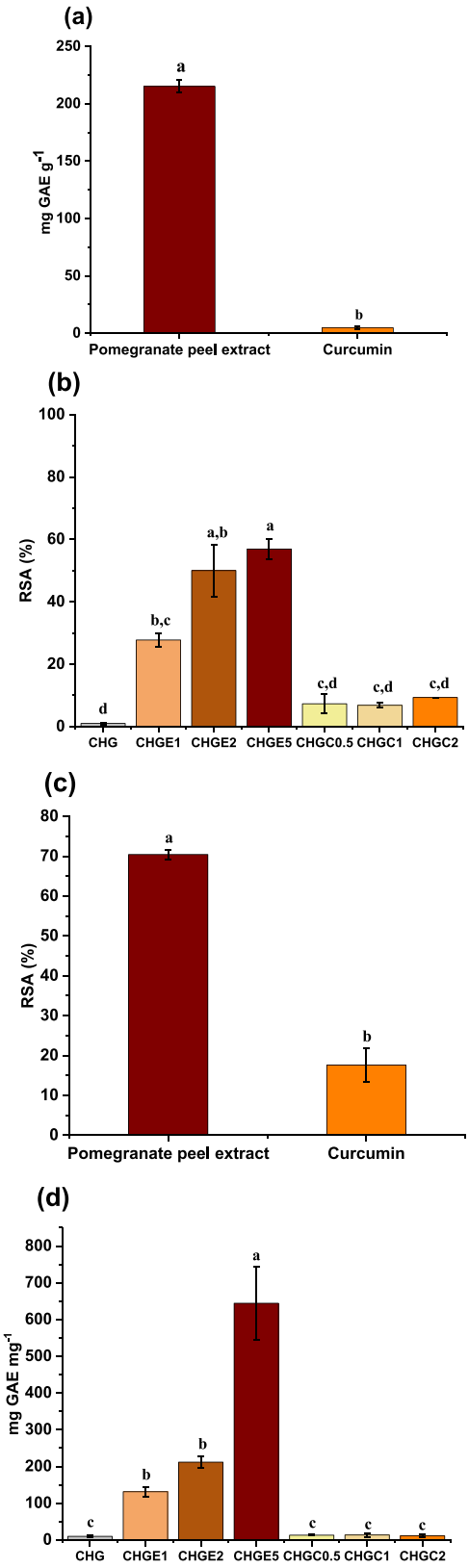

Fig. 6. In A and B, the total phenolic content (TPC) found for pomegranate peel extract and curcumin, as well as for film-forming solutions with chitosan and gelatin; in C and D, the percentages of radical scavenging activity (%RSA) presented by the extract, curcumin, and solutions against the DPPH radical.

concentrations tested, led to a significant increase in the antioxidant activity of the film-forming solutions, compared to CHG (1.00 ± 0.29%); RSA ranged from 27.74 ± 2.17% in CHGE1 to 56.90 ± 3.17% in CHGE5 (Fig. 6d). The solutions containing curcumin, on the other hand, did not reach 10% RSA even at the highest concentration (CHGC2: 9.30 ± 0.01%). Despite the low percentages of inhibition for these solutions, in general all film-forming solutions containing extract and curcumin were able to inhibit more radical than the CHG solution, which shows that the addition of these compounds provided antioxidant activity to the mixture of chitosan and gelatin, improving its active properties.

3.8. Antimicrobial photodynamic tests

The ability of the curcumin- and pomegranate peel extract derivative-films (functionalized on chitosan/gelatin matrix) to inactive bacteria was studied in comparison to chitosan/gelatin films (free of photosensitizers), in light and dark conditions. For that, PDI of planktonic *S. aureus* ATCC 25 923 was performed after immersion of the curcumin- and pomegranate peel extract-functionalized films the bacteria suspension for 10 min. Different photosensitizer concentrations were evaluated using a light source at 450 nm (50 J cm^{-2}) and 525 nm (50 J cm^{-2}), respectively. Fig. 7a shows that curcumin-functionalized films reduce the survival fractions of *S. aureus* up to 4 log units. Moreover, CHG group (chitosan/gelatin) also presented a reduction on *S. aureus* survival due to the intrinsic antimicrobial activity of the chitosan. Fig. 7b presents that solution of pomegranate peel extract (15 mg mL^{-1}) reduces bacterial survival up to 0.7 log unit whereas the

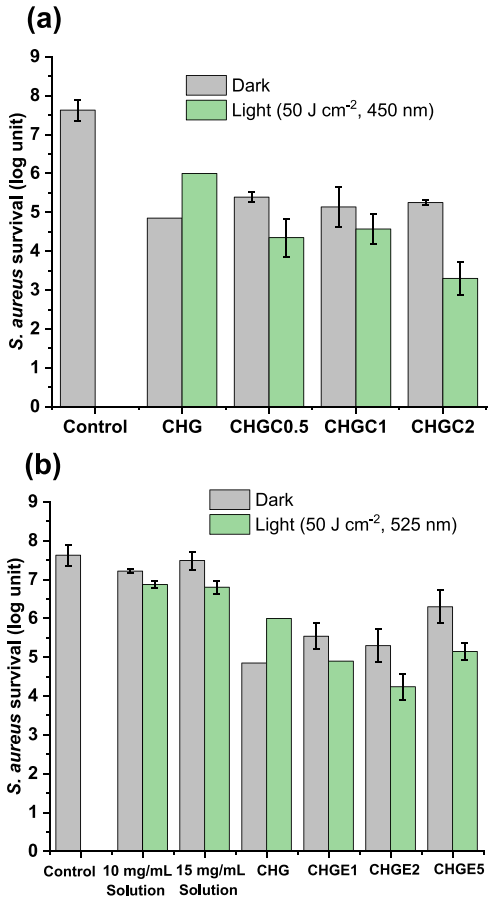

Fig. 7. *S. aureus* survival (log unit): a) curcumin-functionalized films: b) pomegranate peel extract-functionalized films. Each experimental group was performed in duplicate on three separated occasions and the data expressed as mean value (n = 6).

pomegranate-functionalized films showed a *S. aureus* reduction up to 3.5 log units under illumination (50 J cm^{-2}, 525 nm). As previously observed for curcumin-films, pomegranate-functionalized films also presented an antimicrobial effect under dark condition through chitosan antimicrobial action. In addition, the CHGE5 group (the highest concentration of pomegranate) had a lower photoantimicrobial action than the other groups with the lowest concentration of pomegranate, corroborating the results obtained in the photobleaching analysis, which also showed the lowest photodegradation in the presence of light. These experiments demonstrate that the photosensitizers-functionalized films can promote the reduction of adherence/proliferation of bacteria (*S. aureus*) on the chitosan/gelatin matrix by producing ROS. Additionally, the in vitro cytotoxicity towards human cells of the components used (chitosan, gelatin, curcumin, and pomegranate peel extract) on the preparation of the films were evaluated and described in the literature [48–51]. These components presented a good biocompatibility, low cytotoxicity (human fibroblast), and no reduction of human cell growth was observed [48–51].

4. Conclusion

We demonstrated that the physical incorporation of photosensitizing molecules (curcumin and pomegranate peel extract) is an efficient approach to prepare photo- antimicrobial films. The curcumin and pomegranate peel extract chitosan/gelatin-based films characterization by UV–vis, fluorescence, IR spectroscopy, SEM and morphologic analysis (thickness and moisture content, solubility and swelling degree, and opacity) corroborated the effective functionalization of curcumin and pomegranate peel extract onto chitosan/gelation polymer matrix. Our study also revealed that the photosensizers-functionalized chitosan/gelatin-based films show a great photostability/compatibility and a potential use in photoantimicrobial inactivation protocols by photobleaching analysis. Furthermore, these curcumin and pomegranate peel extract chitosan/gelatin-based films presented a significant antimicrobial action reducing *S. aureus* up to 4 log units, using a light dose of 50 J cm^{-2}. The results described herein allow us to foresee the importance of these films as antimicrobial materials, and their potential application for food and medical devices decontamination.

CRediT authorship contribution statement

Conceptualization: Lucas D. Dias, Mirella Romanelli V. Bertolo, Stanislau Bogusz Junior and Vanderlei S. Bagnato; Data curation: Lucas D. Dias, Mirella Romanelli V. Bertolo, Fernanda Alves, Clara M. G. de Faria, Murilo Álison V. Rodrigues, Letícia Keller B. C. Lopes; Formal analysis: Lucas D. Dias, Mirella Romanelli V. Bertolo, Fernanda Alves, Clara M. G. de Faria, Murilo Álison V. Rodrigues, Letícia Keller B. C. Lopes; Funding acquisition: Lucas D. Dias, Mirella Romanelli V. Bertolo, Stanislau Bogusz Junior and Vanderlei S. Bagnato; Investigation: Lucas D. Dias, Mirella Romanelli V. Bertolo, Stanislau Bogusz Junior and Vanderlei S. Bagnato; Methodology: Lucas D. Dias, Mirella Romanelli V. Bertolo, Stanislau Bogusz Junior and Vanderlei S. Bagnato; Project administration: Stanislau Bogusz Junior and Vanderlei S. Bagnato; Resources: Lucas D. Dias, Mirella Romanelli V. Bertolo, Stanislau Bogusz Junior and Vanderlei S. Bagnato; Supervision: Stanislau Bogusz Junior and Vanderlei S. Bagnato; Validation: Ana Maria de Guzzi Plepis, Luiz Henrique C. Mattoso, Stanislau Bogusz Junior and Vanderlei S. Bagnato; Visualization: Lucas D. Dias, Mirella Romanelli V. Bertolo Ana Maria de Guzzi Plepis, Luiz Henrique C. Mattoso, Stanislau Bogusz Junior and Vanderlei S. Bagnato; Roles/Writing - original draft; Writing - review & editing: Lucas D. Dias, Mirella Romanelli V. Bertolo, Stanislau Bogusz Junior and Vanderlei S. Bagnato.

Declaration of Competing Interest

The authors declare that they have no known competing financial

interests or personal relationships that could have appeared to influence the work reported in this paper.

Acknowledgments

The authors thank Fundaç ão de Amparo à Pesquisa do Estado de São Paulo (FAPESP-Brasil) (CEPOF 2013/7276–1) and Instituto Nacional de Ciência e Tecnologia (INCT-Brasil) 'Basic Optics and Applied to Life Sciences' (FAPESP) 2014/50857–8, Conselho Nacional de Desenvolvimento Científico e Tecnológico (CNPq-Brasil) 465 360/2014–9). L.D. Dias thanks Fundaç ão de Amparo à Pesquisa do Estado de São Paulo (FAPESP-Brasil) for his Post-doc Grant 2019/13569–8, and M.R.V. Bertolo thanks Fundaç ão de Amparo à Pesquisa do Estado de São Paulo (FAPESP-Brasil) for her PhD grant (2019/18748–8).

Declaration of interest

The authors declare that they have no known competing financial interests or personal relationships that could have appeared to influence the work reported in this paper. CHGE1 formulation was applied at the Institute of Industrial Property (INPI), number BR 1 020 210 264 047.

Appendix A. Supporting information

Supplementary data associated with this article can be found in the online version at doi:10.1016/j.mtcomm.2022.103791.

References

[1] B. Henderson, An overview of protein moonlighting in bacterial infection, Biochem. Soc. Trans. 42 (2014) 1720–1727.
[2] E. Cerceo, S.B. Deitelzweig, B.M. Sherman, A.N. Amin, Multidrug-Resistant Gram-Negative Bacterial Infections in the Hospital Setting: Overview, Implications for Clinical Practice, and Emerging Treatment Options, Microb. Drug Resist. 22 (2016) 412–431.
[3] L. Delgado, M. Schuster, M. Torero, On the origins of food loss, Appl. Econ. Perspect. Policy 43 (2021) 750–780.
[4] M.M. Elmassry, A. Zayed, M.A. Farag, Gut homeostasis and microbiota under attack: impact of the different types of food contaminants on gut health, Critical Reviews in Food Science and Nutrition.
[5] A. Thakali, J.D. MacRae, A review of chemical and microbial contamination in food: What are the threats to a circular food system? Environ. Res. 194 (2021).
[6] T. Bintsis, Foodborne pathogens, Aims Microbiol. 3 (2017) 529–563.
[7] N. Fegan, I. Jenson, The role of meat in foodborne disease: Is there a coming revolution in risk assessment and management? Meat Sci. 144 (2018) 22–29.
[8] C.R. Arciola, D. Campoccia, L. Montanaro, Implant infections: adhesion, biofilm formation and immune evasion, Nat. Rev. Microbiol. 16 (2018) 397–409.
[9] P.S. Stewart, T. Bjarnsholt, Risk factors for chronic biofilm-related infection associated with implanted medical devices, Clin. Microbiol. Infect. 26 (2020) 1034–1038.
[10] S. Wang, X. Wang, L.M. Yu, M.L. Sun, Progress and trends of photodynamic therapy: From traditional photosensitizers to AIE-based photosensitizers, Photo Photodyn. Ther. 34 (2021).
[11] Z.Y. Liu, H. Zou, Z. Zhao, P.F. Zhang, G.G. Shan, R.T.K. Kwok, J.W.Y. Lam, L. Zheng, B.Z. Tang, Tuning organelle specificity and photodynamic therapy efficiency by molecular function design, Acs Nano 13 (2019) 11283–11293.
[12] P. Thanasekaran, C.H. Chu, S.B. Wang, K.Y. Chen, H.D. Gao, M.M. Lee, S.S. Sun, J. P. Li, J.Y. Chen, J.K. Chen, Y.H. Chang, H.M. Lee, Lipid-wrapped upconversion nanoconstruct/photosensitizer complex for near-infrared light-mediated photodynamic therapy, Acs Appl. Mater. Interfaces 11 (2019) 84–95.
[13] L.D. Dias, K.C. Blanco, I.S. Mfouo-Tynga, N.M. Inada, V.S. Bagnato, Curcumin as a photosensitizer: From molecular structure to recent advances in antimicrobial photodynamic therapy, J. Photochem. Photobiol. C. -Photochem. Rev. 45 (2020).
[14] P. Agostinis, K. Berg, K.A. Cengel, T.H. Foster, A.W. Girotti, S.O. Gollnick, S. M. Hahn, M.R. Hamblin, A. Juzeniene, D. Kessel, M. Korbelik, J. Moan, P. Mroz, D. Nowis, J. Piette, B.C. Wilson, J. Golab, Photodynamic therapy of cancer: an update, Ca-a Cancer J. Clin. 61 (2011) 250–281.
[15] X.Q. Hu, Y.Y. Huang, Y.G. Wang, X.Y. Wang, M.R. Hamblin, Antimicrobial photodynamic therapy to control clinically relevant biofilm infections, Front. Microbiol. 9 (2018).
[16] M. Sharma, A. Dube, S.K. Majumder, Antibacterial photodynamic activity of photosensitizer-embedded alginate-pectin-carboxymethyl cellulose composite biopolymer films, Lasers Med. Sci. 36 (2021) 763–772.
[17] A. Shrestha, A. Kishen, Antibacterial efficacy of photosensitizer functionalized biopolymeric nanoparticles in the presence of tissue inhibitors in root canal, J. Endod. 40 (2014) 566–570.
[18] T. Tsai, H.F. Chien, T.H. Wang, C.T. Huang, Y.B. Ker, C.T. Chen, Chitosan augments photodynamic inactivation of gram-positive and gram-negative bacteria, Antimicrob. Agents Chemother. 55 (2011) 1883–1890.
[19] B. Aaliya, K.V. Sunooj, M. Navaf, P.P. Akhila, C. Sudheesh, S.A. Mir, S. Sabu, A. Sasidharan, M.T. Hlaing, J. George, Recent trends in bacterial decontamination of food products by hurdle technology: a synergistic approach using thermal and non-thermal processing techniques, Food Res. Int. 147 (2021).
[20] A.N. Severyukhina, N.V. Petrova, A.M. Yashchenok, D.N. Bratashov, K. Smuda, I. A. Mamonova, N.A. Yurasov, D.M. Puchinyan, R. Georgieva, H. Baumler, A. Lapanje, D.A. Gorin, Light-induced antibacterial activity of electrospun chitosan-based material containing photosensitizer, Mater. Sci. Eng. C. -Mater. Biol. Appl. 70 (2017) 311–316.
[21] R. Bonnett, M.A. Krysteva, I.G. Lalov, S.V. Artarsky, Water disinfection using photosensitizers immobilized on chitosan, Water Res. 40 (2006) 1269–1275.
[22] A. Shrestha, M.R. Hamblin, A. Kishen, Photoactivated rose bengal functionalized chitosan nanoparticles produce antibacterial/biofilm activity and stabilize dentin-collagen, Nanomed. -Nanotechnol. Biol. Med. 10 (2014) 491–501.
[23] H.X. Wang, F.Y. Ding, L. Ma, Y.H. Zhang, Edible films from chitosan-gelatin: Physical properties and food packaging application, Food Biosci. 40 (2021).
[24] M. Pereda, A.G. Ponce, N.E. Marcovich, R.A. Ruseckaite, J.F. Martucci, Chitosan-gelatin composites and bi-layer films with potential antimicrobial activity, Food Hydrocoll. 25 (2011) 1372–1381.
[25] L.Y. Cai, H. Shi, A.L. Cao, J.Z. Jia, Characterization of gelatin/chitosan ploymer films integrated with docosahexaenoic acids fabricated by different methods, Sci. Rep. 9 (2019).
[26] S. Patel, S. Srivastava, M.R. Singh, D. Singh, Preparation and optimization of chitosan-gelatin films for sustained delivery of lupeol for wound healing, Int. J. Biol. Macromol. 107 (2018) 1888–1897.
[27] A.A. Halim, A. Kamari, E. Phillip, Chitosan, gelatin and methylcellulose films incorporated with tannic acid for food packaging, Int. J. Biol. Macromol. 120 (2018) 1119–1126.
[28] S.S. Cui, H.Y. Chen, H.Y. Zhu, J.M. Tian, X.M. Chi, Z.Y. Qian, S. Achilefu, Y.Q. Gu, Amphiphilic chitosan modified upconversion nanoparticles for in vivo photodynamic therapy induced by near-infrared light, J. Mater. Chem. 22 (2012) 4861–4873.
[29] M. Soltanzadeh, S. Hadi, Peighambardoust Ghanbarzadeh B., S. Amjadi, M. Mohammadi, J.M. Lorenzo, H. Hamishehkar, Active gelatin/cress seed gum-based films reinforced with chitosan nanoparticles encapsulating pomegranate peel extract: preparation and characterization, Food Hydrocoll. 129 (2022), 107620.
[30] M. Soltanzadeh, S.H. Peighambardoust, B. Ghanbarzadeh, M. Mohammadi, J. M. Lorenzo, Chitosan nanoparticles as a promising nanomaterial for encapsulation of pomegranate (Punica granatum L.) peel extract as a natural source of antioxidants, Nanomaterials 11 (2021).
[31] M. Soltanzadeh, S.H. Peighambardoust, B. Ghanbarzadeh, M. Mohammadi, J. M. Lorenzo, Chitosan nanoparticles encapsulating lemongrass (Cymbopogon commutatus) essential oil: Physicochemical, structural, antimicrobial and in-vitro release properties, Int. J. Biol. Macromol. 192 (2021) 1084–1097.
[32] S. Nottagh, J. Hesari, S.H. Peighambardoust, R. Rezaei-Mokarram, H. Jafarizadeh-Malmiri, Effectiveness of edible coating based on chitosan and Natamycin on biological, physico-chemical and organoleptic attributes of Iranian ultra-filtrated cheese, Biologia 75 (2020) 605–611.
[33] M.R.V. Bertolo, Rafael Leme, V.D.C.A. Martins, A.M.D.G. Plepis, S.B. Junior, Rheological characterization of the influence of pomegranate peel extract addition and concentration in chitosan and gelatin coatings, Polysaccharides 2 (2021) 648–660.
[34] M.H. Hosseini, S.H. Razavi, M.A. Mousavi, Antimicrobial, physical and mechanical properties of chitosan-based films incorporated with thyme, clove and cinnamon essential oils, J. Food Process. Preserv. 33 (2009) 727–743.
[35] Y. Peng, Y.F. Li, Combined effects of two kinds of essential oils on physical, mechanical and structural properties of chitosan films, Food Hydrocoll. 36 (2014) 287–293.
[36] V.L. Singleton, R. Orthofer, R.M. Lamuela-Raventos, Analysis of total phenols and other oxidation substrates and antioxidants by means of Folin-Ciocalteu reagent, in: L. Packer (Ed.), Oxid. Antioxid. (Pt A) (1999) 152–178.
[37] D.E. Yoo, K.M. Jeong, S.Y. Han, E.M. Kim, Y. Jin, J. Lee, Deep eutectic solvent-based valorization of spent coffee grounds, Food Chem. 255 (2018) 357–364.
[38] R.P. Singh, K.N.C. Murthy, G.K. Jayaprakasha, Studies on the antioxidant activity of pomegranate (Punica granatum) peel and seed extracts using in vitro models, J. Agric. Food Chem. 50 (2002) 81–86.
[39] M. Kaya, P. Ravikumar, S. Ilk, M. Mujtaba, L. Akyuz, J. Labidi, A.M. Salaberria, Y. S. Cakmak, S.K. Erkul, Production and characterization of chitosan based edible films from Berberis crataegina's fruit extract and seed oil, Innov. Food Sci. Emerg. Technol. 45 (2018) 287–297.
[40] H.X. Hu, X.Y. Yao, Y. Qin, H.M. Yong, J. Liu, Development of multifunctional food packaging by incorporating betalains from vegetable amaranth (Amaranthus tricolor L.) into quaternary ammonium chitosan/fish gelatin blend films, Int. J. Biol. Macromol. 159 (2020) 675–684.
[41] J.J. Zhang, X.W. Huang, X.B. Zou, J.Y. Shi, X.D. Zhai, L. Liu, Z.H. Li, M. Holmes, Y. Y. Gong, M.G. Povey, J.B. Xiao, A visual indicator based on curcumin with high stability for monitoring the freshness of freshwater shrimp, macrobrachium rosenbergii, J. Food Eng. 292 (2021).
[42] X.H. Zhang, Y.T. Li, M.M. Guo, T.Z. Jin, S.A. Arabi, Q. He, B.B. Ismail, Y.Q. Hu, D. H. Liu, Antimicrobial and UV blocking properties of composite chitosan films with curcumin grafted cellulose nanofiber, Food Hydrocoll. 112 (2021).

[43] M.R.V. Bertolo, V.C.A. Martins, M.M. Horn, L.B. Brenelli, A.M.G. Plepis, Rheological and antioxidant properties of chitosan/gelatin-based materials functionalized by pomegranate peel extract, Carbohydr. Polym. 228 (2020).
[44] A. Ghaee, S. Bagheri-Khoulenjani, H.A. Afshar, H. Bogheiri, Biomimetic nanocomposite scaffolds based on surface modified PCL-nanofibers containing curcumin embedded in chitosan/gelatin for skin regeneration, Compos. Part B-Eng. 177 (2019).
[45] S.S. Gharaie, S. Habibi, H. Nazockdast, Fabrication and characterization of chitosan/gelatin/thermoplastic polyurethane blend nanofibers, J. Text. Fibrous Mater. 1 (2018) 1–8.
[46] J.S. Dysart, G. Singh, M.S. Patterson, Calculation of singlet oxygen dose from photosensitizer fluorescence and photobleaching during mTHPC photodynamic therapy of MLL cells, Photochem. Photobiol. 81 (2005) 196–205.
[47] I. Georgakoudi, T.H. Foster, Singlet oxygen- versus nonsinglet oxygen-mediated mechanisms of sensitizer photobleaching and their effects on photodynamic dosimetry, Photochem. Photobiol. 67 (1998) 612–625.
[48] Z.U. Aydin, K.E. Akpinar, C. Hepokur, D. Erdonmez, Assessment of toxicity and oxidative DNA damage of sodium hypochlorite, chitosan and propolis on fibroblast cells, Braz. Oral. Res. 32 (2018) 1–8.
[49] A.K. Gupta, M. Gupta, S.J. Yarwood, A.S.G. Curtis, Effect of cellular uptake of gelatin nanoparticles on adhesion, morphology and cytoskeleton organisation of human fibroblasts, J. Control. Release 95 (2004) 197–207.
[50] S.K. Sukumaran, R.J. Vadakkekitical, H. Kanakath, Comparative evaluation of the effect of curcumin and chlorhexidine on human fibroblast viability and migration: An in vitro study, J. Indian Soc. Periodo 24 (2020) 109–116.
[51] H. Cheshomi, A.A. Bahrami, H. Rafatpanah, M.M. Matin, The effects of ellagic acid and other pomegranate (Punica granatum L.) derivatives on human gastric cancer AGS cells, Hum. Exp. Toxicol. 41 (2022) 1–16.